

Conversion of just-continuous metallic films to large particulate substrates for metal-enhanced fluorescence

Kadir Aslan, Stuart N. Malyn, Yongxia Zhang, and Chris D. Geddes^{a)}

Institute of Fluorescence, Laboratory for Advanced Medical Plasmonics and Laboratory for Advanced Fluorescence Spectroscopy, Medical Biotechnology Center, University of Maryland Biotechnology Institute, 725 W. Lombard St., Baltimore, Maryland 21201, USA

(Received 29 October 2007; accepted 11 February 2008; published online 25 April 2008)

We report the effects of thermally annealing, non-, *just*-, and thick continuous silver films for their potential applications in metal-enhanced fluorescence, a near-field concept which can alter the free-space absorption and emissive properties of close-proximity fluorophores (excited states). We have chosen to anneal a noncontinuous particulate film 5 nm thick and two thicker continuous films, 15 and 25 nm thick, respectively. Our results show that the annealing of the 25 nm film has little effect on close-proximity fluorescence when coated with a monolayer of fluorophore-labeled protein. However, the 15 nm continuous film *cracks* upon annealing, producing large nanoparticles which are ideal for enhancing the fluorescence of close-proximity fluorophores that are indeed difficult to prepare by other wet-chemical deposition processes. The annealing of 5 nm noncontinuous particulate films (a control sample) has little influence on metal-enhanced fluorescence, as expected. © 2008 American Institute of Physics. [DOI: 10.1063/1.2905319]

I. INTRODUCTION

In recent years, our laboratory has both described and demonstrated many favorable photophysical effects of electronically excited states (fluorophores/luminophores) in close proximity to plasmon resonant particles.¹⁻³ In these examples of metal-enhanced fluorescence (MEF), it has become apparent that the true mechanism for MEF is far more elegant than the simple radiative decay rate description postulated by others,⁴ and is in fact underpinned by the formation of a mirror dipole on the metallic nanoparticle, which itself radiates highly efficiently, effectively resulting in an enhanced luminescence.^{3,5-7} The coupled fluorophore lifetime is also observed to be much shorter than the “free-space lifetime,” reflecting the very fast “plasmon” lifetime of the coupled quanta.⁵⁻⁷ Further, it is thought that the MEF effect is a consequence of an excited state coupling with the scattering mode of nanoparticles, which is thought to account for very fast MEF lifetimes, i.e., a coupled elastic scattering event.^{3,8} For metallic nanoparticles, the extinction spectrum is comprised of both absorption and scattering components.⁹ For smaller particles (<25 nm), then the extinction is for the most part dominated by absorption, while for larger particles, by scattering. For a fixed wavelength, this scales as the radius cubed and to the sixth power, respectively.⁹ Given that MEF is thought to be the ability of a nanoparticle to plasmon scatter coupled quanta (i.e., fluorescence, phosphorescence, etc.),³ then concordantly larger particles have subsequently been shown to be ideal for MEF.^{3,8} It is this train of thought which readily accounts for the numerous reports of *luminescence quenching* by small metallic nanoparticles. While our mechanism for MEF is described very recently,³ we have reported compelling data in the past. In these reports, (i)

MEF is seen to be more pronounced for larger particles, (ii) the wavelength dependence of MEF suggests a correlation between the scattering spectra of the nanoparticles and the emission spectra of the fluorophores, (iii) MEF is angular dependent,¹⁰ both from an observation and excitation perspective, similar to scattering by nanoparticles themselves,¹¹ (iv) metals that are ideal for MEF are those with high free electron densities,¹² and (v) continuous metallic films have been shown to couple fluorophore emission, when fluorophores are positioned at less than 100 nm from the surface. In addition, the coupled emission in (v) has been shown to be completely *p* polarized, strongly indicating that the coupled-plasmon system is radiating.^{13,14}

Silver is usually the noble metal of choice^{12,15-17} for applications in MEF and surface-enhanced Raman spectroscopy. The preparation of silvered substrates include several modes of deposition, such as by wet chemistry,¹⁸ a layer-by-layer deposition technique,¹⁹ electrochemically,²⁰ on glass,²¹ plastic substrates,²² and on indium tin oxide.²³ One of the most commonly used techniques is vapor deposition^{21,24-27} as it yields the most reproducible substrates among the deposition techniques aforementioned. After the deposition of silver films onto substrates, a high-temperature postannealing process can also be applied to introduce a quasiperiodic roughness that further increases the utility of these surfaces.^{21,28,29}

Subsequently, in this paper, we investigate the effect on MEF of thermally annealed non-, *just*-, and thick continuous films. Silver films ≈ 15 nm thick readily reflect visible light, their absorption/transmission spectra not unlike a conventional thin optical silver mirror. However, when thermally annealed in the absence of oxygen, the films “crack” (*globulate*), producing very large nanoparticles, which are somewhat difficult to grow/produce by other wet-chemical deposition techniques, without forming a continuous film. Hence,

^{a)}Author to whom correspondence should be addressed. Electronic mail: geddes@umbi.umd.edu.

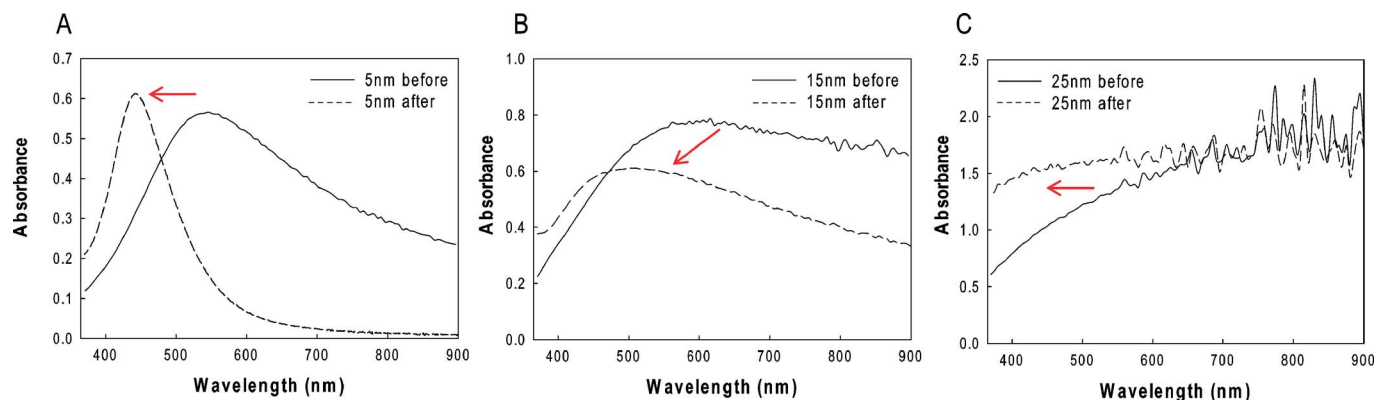


FIG. 1. (Color online) Absorption spectrum of (A) 5 nm, (B) 15 nm, and (C) 25 nm thick silver films deposited onto amine-coated glass microscope slides before and after annealing at 200 °C for 1 h. The oven was nitrogen purged. The arrows indicate the blueshift in the surface plasmon resonance peak of silver after annealing.

we have investigated the annealing of just-continuous silver films primarily for applications in MEF. Our results demonstrate that annealed just-continuous films are ideal substrates for MEF, producing ≈ 30 -fold enhancements in fluorescence, which appear more suitable than the much smaller SiFs, common substrates used for MEF.²

II. EXPERIMENTAL SECTION

A. Materials

Silver wire (99.999%), standard microscope slides and Fluorescein isothiocyanate (FITC-HSA) were purchased from Sigma-Aldrich. Nanopure water (>18.0 M Ω) purified using a Millipore Milli-Q gradient system was used in all experiments.

B. Preparation of thick silver films by vacuum vapor deposition

Thick silver films (TSFs) were deposited in a consolidated vacuum vapor deposition system (model 306, BOC Edwards). Glass slides were pretreated by air plasma under 1×10^{-4} mbar for 3 min before depositing the metal film. The silver wire was melted on the filament, evaporated under a pressure of $<1 \times 10^{-7}$ mbar, and deposited onto the glass slides. The deposition rate was adjusted by the filament current (1 Å/s), and the thickness of film was measured with a quartz crystal microbalance positioned close to the glass substrate within the deposition chamber.

C. Annealing of TSFs

Annealing of TSFs was performed in a Fisher scientific vacuum oven (model 280A) at 200 °C for 1 h. Trace amounts of oxygen in the oven were eliminated by alternately purging the oven with ultrahigh purity nitrogen (Air-gas, MD) and pumping down to vacuum four times for 10 min, before the annealing process commenced.

D. MEF from TSFs

Binding the FITC-HSA to both the annealed and unannealed TSFs was accomplished by spotting the slide with a 10 μ M FITC-HSA solution and allowing to air dry, followed

by rinsing with water to remove the unbound material. HSA is known to passively adsorb to noble metal surfaces and form an ≈ 4 nm thick protein monolayer,³⁰ allowing us to study the fluorescence spectral properties of noncovalent FITC-HSA complexes before and after annealing. By equally coating a TSF with FITC-HSA, we were also able to determine the enhancement factor (benefit) obtained from using the silver, i.e., (intensity on silver/intensity on unsilvered glass) and the enhancement factor (benefit) obtained from using *annealed/unannealed* silver surfaces, given that all surfaces are known to have an approximately equal to monolayer protein coverage. In addition, this sample format is a characteristic of MEF-based immunoassays, a growing application for both MEF and silvered surfaces.³¹

E. Angular-dependent light scattering and fluorescence measurements

The angular-dependent light scattering and fluorescence intensity of FITC-HSA on annealed silver films of various thicknesses were measured using an X-Y rotating stage (Edmund Optics) that was modified to hold a standard 75×25 mm² microscope slide, with a fiber optic mount. TSFs were illuminated with a polarized laser source at 473 nm, a neutral density filter being used to attenuate the laser intensity. The emission was observed through a 488 nm long-pass filter (Edmund Optics). The angular-dependent polarized *scattered light* from the TSFs was collected through a dichroic sheet polarizer (Edmund Optics) into a 600 μ m broad wavelength fiber that was connected to an Ocean Optics HD2000 spectrofluorometer. The photostability of FITC-HSA on TSFs under constant illumination with a 473 nm laser source was observed by simply measuring the emission at 225° and 340° for 10 min.

The real-color photographs of FITC-HSA on nonsilvered glass slides and TSFs were taken with a Canon digital camera (S1-IS, 3.2 Mpixel, 10 \times optical zoom) using the same long-pass filter that was used for the emission spectra.

III. RESULTS AND DISCUSSION

Figure 1 shows the absorption spectrum of 5, 15, and 25 nm TSFs deposited onto amine-coated glass microscope

slides both before and after annealing at 200 °C for 1 h in the absence of oxygen. While 5 and 15 nm TSFs showed a surface plasmon resonance (SPR) peak at ≈ 580 nm before annealing and have a broad absorption at longer wavelengths, 25 nm TSF did not show a SPR peak. This is thought to be due to the fact that evaporated silver films on substrates often become globular films and as the thickness is increased, the distance between the globular particles is decreased, resulting in collective coupled oscillations of surface plasmons at longer wavelengths, and thus, a broad absorption spectrum is observed, similar to that of a silver mirror. After annealing the silver films at 200 °C for 1 h, the SPR peaks for 5 and 15 nm TSFs blueshifted to ≈ 440 and ≈ 480 nm, respectively. Moreover, a narrowing of the absorption spectrum at longer wavelengths is also observed for 5 and 15 nm TSFs after annealing, which indicates that the distance between the globular silver particles is further increased by postannealing. In contrast, annealing of the 25 nm TSF did not result in the appearance of any SPR peak, indicating that there was little or no change in the morphology of the thick silver film.

We note that the reproducibility of the annealing of TSFs depends mostly on two factors: (i) the deposition rate of TSFs on the glass microscope slides and (ii) the annealing temperature and time. Given the deposition of TSFs on glass substrates is an established method and is therefore very reproducible, and the fact that the annealing process commences after nitrogen purging at the annealing temperature, then one can produce reproducible TSFs.

Previous studies on the morphological changes in vapor deposited TSFs on Si wafer after annealing revealed that the change in the morphology of the TSFs is temperature dependent.^{28,29} It was shown that a 6 nm TSF appearing as globular structures on a Si wafer before annealing, starts to break up at an annealing temperature of 100 °C, the particles becoming larger and further separated from one another at 200 °C, and become even more pronounced at even higher annealing temperatures.²⁸ Similar results were also reported for 5–30 nm thick gold films, where the annealing of gold films at 240 °C resulted in the formation of larger globular structures of gold as the distance between gold globular structures is increased.^{29,32} In this regard, it is important to note that our choice of thicknesses of 5, 15, and 25 nm silver films are based on the following: *before annealing* (i) 5 nm TSF is considered to be a noncontinuous film (i.e., particulate) and is expected to show MEF before annealing,³³ (ii) 15 nm TSF is considered to be a just-continuous film (at the deposition rate we used) and is not expected to show MEF, and (iii) 25 nm TSF is considered to be a continuous films and is expected not to show MEF before or even after annealing. The appearance of a SPR peak for 15 nm thick films after annealing, as we have shown in our absorption measurements, led us to believe that just-continuous 15 nm TSFs could be converted into efficient substrates for MEF applications, after a postannealing process, a highly attractive notion, given the difficulties of producing large particulate films by wet-chemical deposition processes without forming continuous films. Our hypothesis for the conversion of just-continuous TSFs for the applications in MEF is consistent

with the work previously published by Feafanov *et al.*²¹ who has reported the conversion of ≈ 14 nm TSFs as more efficient SERS substrates as compared to as-deposited TSFs.

According to the previously described unified plasmon-fluorophore theory (UPFT),³ MEF is related to the surface plasmons' ability to scatter the fluorophore's coupled emission (larger particles scatter more efficiently) and is therefore thought to be somewhat angular-dependent.³⁴ Since MEF from plasmonic particle-deposited surfaces (as deposited from a premade solution³⁴ or prepared using an annealing process⁸) is more pronounced as the size of the particles increases, we systematically studied the angular-dependent scattering of light (plasmon scattering) and fluorescence emission from the 5, 15, and 25 nm TSFs before and after annealing at 200 °C. Figure 2(a) shows polar plots for scattering of 473 nm laser light by a 5 nm TSF deposited on a glass microscope slide before and after annealing. As expected, we observe an angular-dependent scattering of laser light by 5 nm TSF before annealing, which is slightly increased in intensity after annealing at 200 °C. We attribute this observation to the increase in height (size) of the silver particles (from an average height of 5–10 nm), as confirmed by atomic force microscopy (AFM) [supplementary Fig. 1 (Ref. 35)] combined with the increase in distance between the particles that we infer from the absorption spectra [Fig. 1(a), we note that mass is conserved on the surface during annealing, the particles grow in size but decrease in number. The spacing between the particles also increases, as confirmed by AFM analysis]. It is also important to note that while the increase in particle height (size) results in increased scattering intensities, the larger distances between the particles as a result of the annealing process *partially* offsets this effect (to the extent that we were unable to quantify here), and thus, a slight increase in the overall angular-dependent scattering intensities is observed for 5 nm TSF.

Figures 2(b) and 2(c) show the polar plots for fluorescence emission and the fluorescence spectra measured at an angle of 225° from FITC-HSA coated onto 5 nm TSF before and after annealing, respectively. We observed *similar* angular-dependent fluorescence emission intensities from 5 nm TSFs, both before and after annealing, as also shown by the emission spectra measured at an observation angle of 225°. Further, visual evidence for similar fluorescence emission from FITC-HSA coated onto 5 nm TSFs are presented in the real-color photographs shown in the bottom of Fig. 2(c). We note that the angular-dependent fluorescence emission pattern for 5 nm TSF after the annealing process is *similar* to the angular-dependent scattering of light by the plasmonic structures themselves, although we note that the presence of the glass substrate also makes a significant contribution to the angular dependent emission observed.¹⁰ (Note: our fluorophores are heterogeneously distributed on both glass and silver). These results are consistent with UPFT where a fluorophore's excited state is thought to couple to surface plasmons and subsequently scatter at the same wavelength elastically and in an angular-dependent fashion.^{3–10}

Figure 3(a) shows the polar plots for scattering of 473 nm light by a 15 nm TSF from a glass microscope slide,

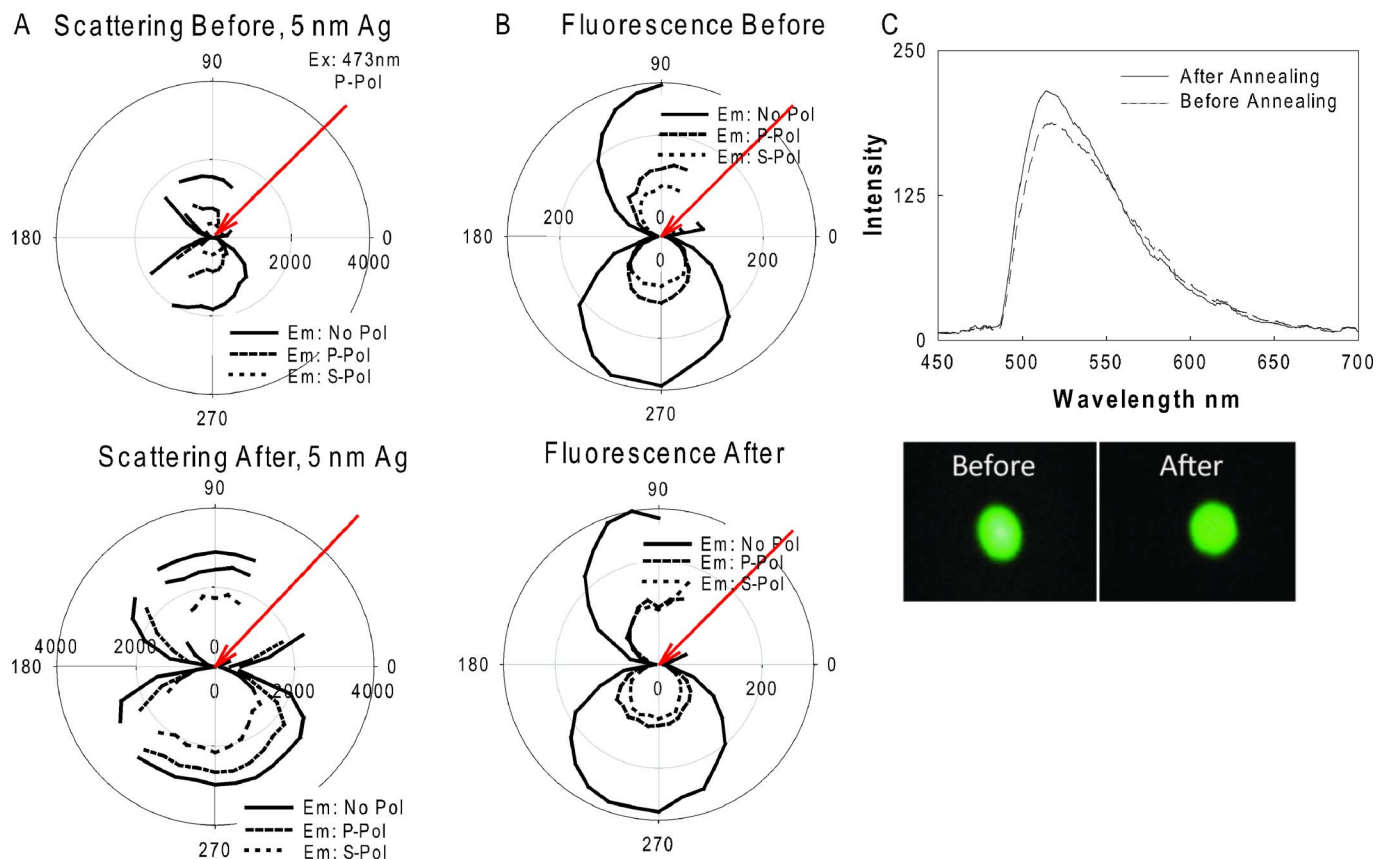


FIG. 2. (Color online) Results for 5 nm thick silver films before (top row) and after (bottom row) annealing at 200 °C for 1 h in a vacuum oven: (A) polar plots for scattering of 473 nm laser light, (B) polar plots for fluorescence emission from FITC-HSA coated onto thick silver films, and (C) fluorescence emission spectrum measured at 225° and the real-color photographs of emission from FITC-HSA coated onto silver films. No pol: no polarization, *p* pol: *p* polarization, *s* pol: *s* polarization.

both before and after annealing. While the angular-dependent scattering of light from 15 nm TSF is similar to that from a thin reflective surface (mirror) before annealing, the angular-dependent light scattering pattern becomes similar to that from a surface that contains large nanoparticles, after the annealing process, [bottom of Fig. 3(a)]. We confirm this assumption through (1) absorption measurements where we observed the appearance of the SPR peak for silver after annealing [Fig. 1(b)] (2) AFM analysis, where the globular silver particles are clearly seen [supplemental Fig. 2 (Ref. 35)], and finally (3) angular-dependent light scattering, where the annealed 15 nm TSF scatter light similar to large silver nanoparticles [bottom of Fig. 3(a)].

Figures 3(b) and 3(c) show the polar plots of fluorescence emission and fluorescence spectra measured at 225° from FITC-HSA coated onto 15 nm TSF before and after annealing, respectively. We note that both the fluorescence polar plots and photographs were taken through an emission filter. While we observe no fluorescence emission at all observation angles from a 15 nm TSF *before annealing*, angular-dependent fluorescence emission from annealed 15 nm TSF can readily be observed. A snapshot of fluorescence emission at an observation angle of 225° shows visual evidence of the significantly larger fluorescence emission from FITC-HSA coated onto annealed 15 nm TSFs [Fig. 3(c) (enhancement factor=30-fold)]. We note that angular-dependent fluorescence emission shown in Fig. 3(b) is simi-

lar to the angular-dependent scattering of light by the annealed 15 nm TSF, which supports UPFT.³ These results indicate that a just-continuous silver film can be “cracked” or “globulated” and made noncontinuous, to produce very large particles, which are somewhat difficult to grow and deposit by wet-chemical deposition techniques and can therefore be utilized for downstream applications in MEF.

To show that the enhancement of fluorescence is facilitated through the coupling of a fluorophore’s dipole to surface plasmons and not due to random scattering of light by metallic surfaces or indeed other mechanisms, we additionally studied a much thicker TSF, where under our conditions, the thick film cannot support surface plasmons. In this regard, we measured the angular-dependent light scattering and angular-dependent fluorescence emission from 25 nm TSFs both before and after annealing (Fig. 4). Figure 4(a) shows the polar plots for scattering of 473 nm laser light by 25 nm TSF on a glass microscope slide both before and after annealing. While the angular-dependent scattering of light from 25 nm TSF is similar to that from a thin reflective surface (mirror) before annealing, where the light is mostly reflected, after the annealing process the angular-dependent light scattering pattern shows a slightly broader forward scattering profile but the majority of light is still scattered into the back excitation half-space. AFM analysis of the 25 nm TSF before and after annealing reveals the continuous film nature as also confirmed by the absorption spectra shown in Fig. 1. Figure

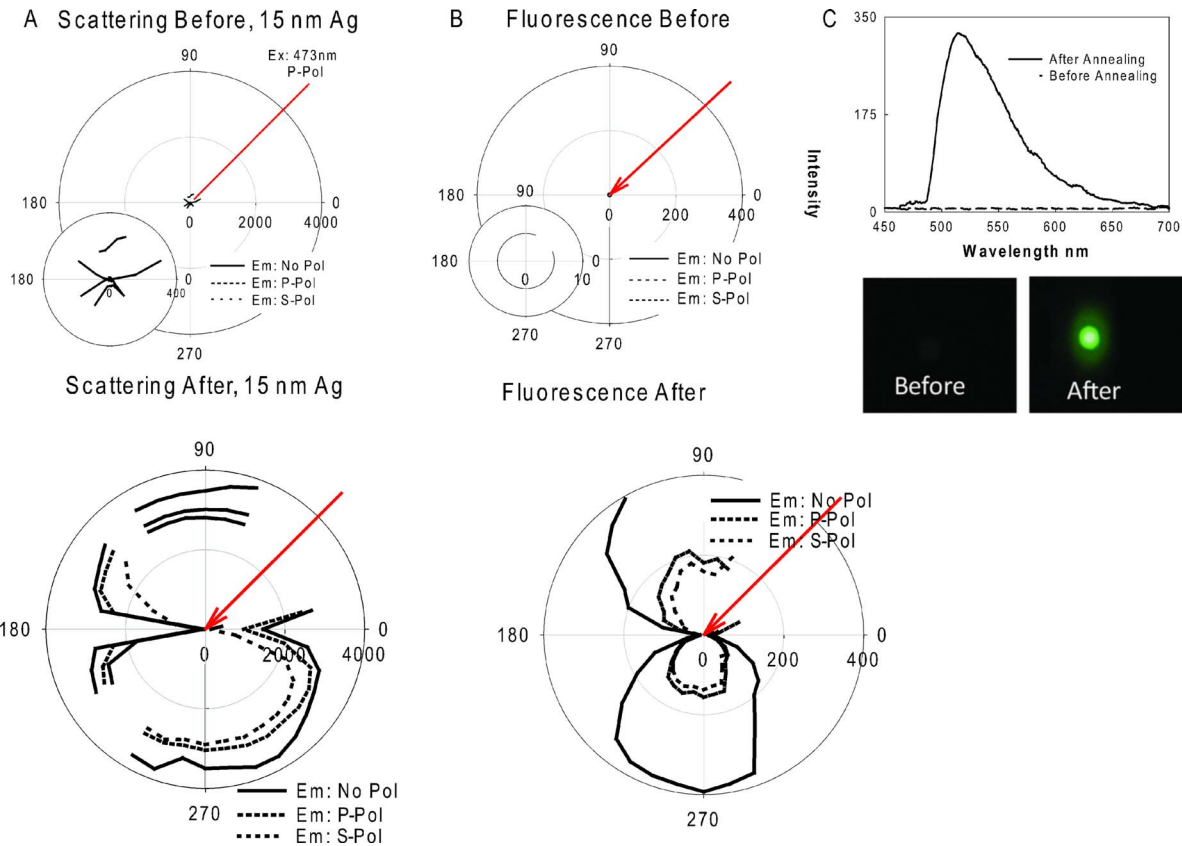


FIG. 3. (Color online) Results for 15 nm thick silver films before (top row) and after (bottom row) annealing at 200 °C for 1 hour in a vacuum oven: (A) polar plots for scattering of 473 nm excitation light, (B) polar plots for fluorescence emission from FITC-HSA coated onto silver films, and (C) fluorescence emission spectrum measured at 225 degrees and real-color photograph of emission from FITC-HSA coated onto silver films. No Pol-No Polarization, *P* Pol: *p*-polarization, *S* Pol: *s*-polarization.

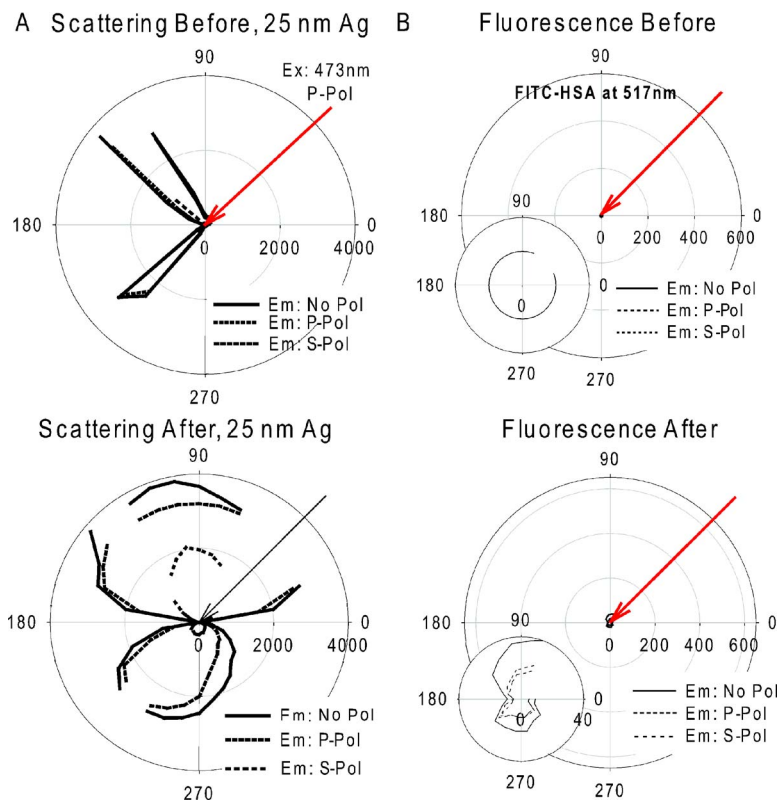


FIG. 4. (Color online) Polar plots for 25 nm thick silver films before (top row) and after (bottom row) annealing at 200 °C for 1 hour in a vacuum oven: (A) scattering of 473 nm excitation light and (B) fluorescence emission from FITC-HSA coated onto silver films measured at 225°. No Pol-No Polarization, *P* Pol: *p*-polarization, *S* Pol: *s*-polarization.

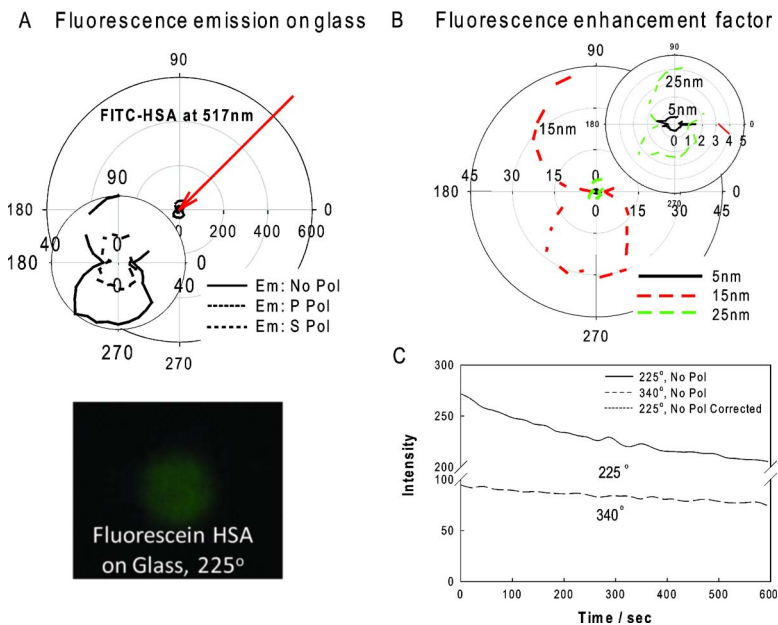


FIG. 5. (Color online) Polar plots for (A) fluorescence emission from FITC-HSA coated glass slides and (B) fluorescence enhancement factor, i.e., the ratio of emission intensity of FITC-HSA at 517 nm on silver films, after annealing and the emission intensity of FITC-HSA on glass slides measured at 225 degrees. (C) Photostability of FITC-HSA measured at 225 and 340 degrees on a 15 nm annealed silver film. A separate experiment, where the initial emission intensity at 225 degrees was matched to the steady-state emission intensity at 340 degrees by reducing the excitation intensity with a neutral density filter, was also undertaken. Real-color photographs show the fluorescence emission from FITC-HSA taken through a 532 nm emission filter at 225 degrees. No Pol-No Polarization, *P* Pol: *p*-polarization, *S* Pol: *s*-polarization.

4(b) shows the polar plots of fluorescence emission from FITC-HSA coated onto 25 nm TSF before and after annealing. As expected, we observe little to no fluorescence signal from the 25 nm TSFs both before and after annealing. These results indicate that 25 nm TSFs cannot be converted using our procedures, into substrates for applications in MEF and, moreover, that under the conditions used here, the continuous films cannot support a SPR, an important criterion for MEF.³

In order to quantitate the ability of TSFs for MEF, we measured the angular-dependent fluorescence intensity from FITC-HSA coated onto a control sample substrate that does not contain TSFs and compared our results to the fluorescence emission intensities obtained for annealed TSFs, as shown in Figs. 5(a) and 5(b). Angular-dependent fluorescence emission and a real-color photograph for fluorescence emission taken at 225° from a FITC-HSA coated glass microscope slide both show the very weak fluorescence emission from the glass substrate [Fig. 5(a), a control sample]. Figure 5(b) shows the fluorescence enhancement factor, i.e., the ratio of emission intensity of FITC-HSA at 517 nm on annealed TSFs and the emission intensity of FITC-HSA on glass slides measured at 225°. The fluorescence emission intensity from annealed 15 nm TSF is up to 30-fold larger as compared to the control glass surface, while the fluorescence emission is eightfold larger for annealed 5 nm TSF. No enhanced fluorescence is observed from the annealed 25 nm TSF, as expected.³

We have previously shown that the photostability of fluorophores near plasmonic nanoparticles varies with the angle of observation (degree of fluorophore coupling),³⁴ which arises from the fact that the scattering of light and fluorescence enhancement both vary with the angle of observation. In this paper, we have also measured the photostability of FITC-HSA at 225° (in the direction of propagation of the incident light) and 340° (away from the direction of the propagation) on 15 nm annealed TSF. A separate experiment, where the initial emission intensity at 225° was matched to

the initial steady-state emission intensity at 340° by reducing the excitation intensity with a neutral density filter, was also undertaken. We observe that the photostability of FITC, indeed, depends slightly on the observation angle providing with us additional evidence that both MEF and enhanced fluorophore photostabilities can be observed from annealed 15 nm TSF [Fig. 5(c)].

IV. CONCLUSIONS

In this paper, we have investigated the effects of high-temperature annealing on TSFs and have shown that annealed 15 nm TSFs can be used for potential applications in MEF. TSFs with film thicknesses of 5, 15, and 25 nm were deposited onto glass substrates using the thermal vapor deposition technique that resulted in noncontinuous particulate films, a just-continuous film, and a thick continuous film, respectively. The surface morphological changes on TSFs induced by the annealing process, carried out at 200 °C for 1 h, were followed by absorption spectroscopy, AFM, and angular-dependent light scattering and fluorescence techniques. After annealing, we observed an increase in the height (size) of the 5 nm TSFs, as the separation distance between the particles also increased. We also observed a little change in MEF for 5 nm TSFs as a result of annealing. The annealing of 15 nm TSFs resulted in the conversion of the just-continuous films into large globular particles with a SPR peak around ≈ 480 nm and, subsequently, these surfaces yielded up to 30-fold enhancement in fluorescence emission. Much thicker TSFs (25 nm) that showed no SPR peak both before and after annealing, were not beneficial for MEF, confirming our hypothesis that silver films ≈ 15 nm thick can be annealed to produce large particulate films, not readily assessable by other chemical deposition techniques.

ACKNOWLEDGMENTS

This work was supported by the Middle Atlantic Regional Center of Excellence for Biodefense and Emerging

Infectious Diseases Research (NIH NIAID U54 AI057168) and the National Institute of Neurological Disorders & Stroke (NIH) Grant No. NS055187-01A2. The authors would like to thank UMBI, MBC, and the IoF also for salary support.

- ¹C. D. Geddes and J. R. Lakowicz, *J. Fluoresc.* **12**, 121 (2002).
- ²K. Aslan, I. Gryczynski, J. Malicka, E. Matveeva, J. R. Lakowicz, and C. D. Geddes, *Curr. Opin. Biotechnol.* **16**, 55 (2005).
- ³K. Aslan, M. J. R. Previte, Y. X. Zhang, and C. D. Geddes, *Biophys. J.*, abstract, 371A (2007).
- ⁴J. R. Lakowicz, *Anal. Biochem.* **298**, 1 (2001).
- ⁵Y. Zhang, K. Aslan, M. J. Previte, and C. D. Geddes, *Chem. Phys. Lett.* **432**, 528 (2006).
- ⁶M. H. Chowdhury, K. Aslan, S. N. Malyn, J. R. Lakowicz, and C. D. Geddes, *Appl. Phys. Lett.* **88**, 173104 (2006).
- ⁷Y. Zhang, K. Aslan, M. J. Previte, and C. D. Geddes, *Appl. Phys. Lett.* **90**, 053107 (2007).
- ⁸K. Aslan, Z. Leonenko, J. R. Lakowicz, and C. D. Geddes, *J. Fluoresc.* **15**, 643 (2005).
- ⁹J. Yguerabide and E. E. Yguerabide, *Anal. Biochem.* **262**, 137 (1998).
- ¹⁰K. Aslan, S. N. Malyn, and C. D. Geddes, *Analyst (Cambridge, U.K.)* **132**, 1112 (2007).
- ¹¹K. Aslan, P. Holley, L. Davies, J. R. Lakowicz, and C. D. Geddes, *J. Am. Chem. Soc.* **127**, 12115 (2005).
- ¹²Y. Zhang, K. Aslan, M. J. R. Previte, and C. D. Geddes, *Appl. Phys. Lett.* **90**, 173116 (2007).
- ¹³M. H. Chowdhury, S. N. Malyn, K. Aslan, J. R. Lakowicz, and C. D. Geddes, *J. Phys. Chem. B* **110**, 22644 (2006).
- ¹⁴M. J. R. Previte, K. Aslan, Y. X. Zhang, and C. D. Geddes, *J. Phys. Chem. C* **111**, 6051 (2007).
- ¹⁵C. Zhang, K. Abdjalilov, and H. Grebel, *J. Chem. Phys.* **127**, 044701 (2007).
- ¹⁶K. R. Strehle, D. Cialla, P. Rosch, T. Henkel, M. Kohler, and J. Popp, *Anal. Chem.* **79**, 1542 (2007).
- ¹⁷Q. Yu and G. Golden, *Langmuir* **23**, 8659 (2007).
- ¹⁸K. Aslan, J. Huang, G. M. Wilson, and C. D. Geddes, *J. Am. Chem. Soc.* **128**, 4206 (2006).
- ¹⁹D. S. dos Santos and R. F. Aroca, *Analyst (Cambridge, U.K.)* **132**, 450 (2007).
- ²⁰C. D. Geddes, A. Parfenov, D. Roll, J. Y. Fang, and J. R. Lakowicz, *Langmuir* **19**, 6236 (2003).
- ²¹A. Feofanov, A. Ianoul, E. Kryukov, S. Maskevich, G. Vasiliuk, L. Kivach, and I. Nabiev, *Anal. Chem.* **69**, 3731 (1997).
- ²²K. Aslan, P. Holley, and C. D. Geddes, *J. Mater. Chem.* **16**, 2846 (2006).
- ²³H. J. Park, D. Vak, Y. Y. Noh, B. Lim, and D. Y. Kim, *Appl. Phys. Lett.* **90**, 161107 (2007).
- ²⁴D. S. Dunn, N. Sridhar, M. A. Miller, K. T. Price, R. Pabalan, and T. A. Abrajano, Jr., *Appl. Spectrosc.* **61**, 25 (2007).
- ²⁵H. Li and B. M. Cullum, *Appl. Spectrosc.* **59**, 4107 (2005).
- ²⁶M. Kawasaki and S. Mine, *J. Phys. Chem. B* **109**, 17254 (2005).
- ²⁷M. Kawasaki and S. Mine, *Chem. Lett.* **34**, 1038 (2005).
- ²⁸Y. Suzuki, Y. Ojima, Y. Fukui, H. Fazyia, and K. Sagisaka, *Thin Solid Films* **515**, 3073 (2007).
- ²⁹N. Strekal, A. Maskevich, S. Maskevich, J. C. Jardillier, and I. Nabiev, *Biopolymers* **57**, 325 (2000).
- ³⁰L. Hao and J. Lawrence, *Colloids Surf., B* **34**, 87 (2004).
- ³¹K. Aslan and C. D. Geddes, *Plasmonics* **1**, 53 (2006).
- ³²I. Doron-Mor, Z. Barkay, N. Filip-Granit, A. Vaskevich, and I. Rubinstein, *Chem. Mater.* **16**, 3476 (2004).
- ³³C. D. Geddes, H. Cao, I. Gryczynski, Z. Gryczynski, J. Fang, and J. R. Lakowicz, *J. Phys. Chem. A* **107**, 3443 (2003).
- ³⁴K. Aslan, S. N. Malyn, and C. D. Geddes, *J. Fluoresc.* **17**, 7 (2007).
- ³⁵See EPAPS Document No. E-JAPIAU-103-051808 for AFM images of annealed thick silver films. For more information on EPAPS, see <http://www.aip.org/pubservs/epaps.html>.